

# Local Moment Formation in the Superconducting State of a Doped Mott Insulator

Ziqiang Wang<sup>a</sup> and Patrick A. Lee<sup>b</sup>

<sup>a</sup>*Department of Physics, Boston College, Chestnut Hill, MA 02467*

<sup>b</sup>*Department of Physics, Massachusetts Institute of Technology, Cambridge, MA 02139*

(December 2, 2024)

A microscopic theory is presented for the local moment formation near a non-magnetic impurity or a copper defect in high- $T_c$  superconductors. We use a renormalized meanfield theory of the  $t - J$  model for a doped Mott insulator and study the fully self-consistent, spatially unrestricted solutions of the d-wave superconducting (SC) state in both the spin  $S = 0$  and  $S = 1/2$  sectors. We find a transition from the singlet d-wave SC state to a spin doublet SC state when the renormalized exchange coupling exceeds a doping dependent critical value. The induced  $S = 1/2$  moment is staggered and localized around the impurity. It arises from the binding of an  $S = 1/2$  nodal quasiparticle excitation to the impurity. The local density of states spectrum is calculated and connections to NMR and STM experiments are discussed.

PACS numbers: 74.25.Jb, 74.25.Ha, 75.20.Hr, 74.20.Mn

The local electronic structure near non-magnetic impurities in high- $T_c$  superconductors has attracted wide attention recently. A series of NMR experiments in  $\text{YBa}_2\text{Cu}_3\text{O}_{7-x}$  (YBCO) have shown that with the substitution of nonmagnetic Zn/Li for the Cu atoms in the  $\text{CuO}_2$  plane, an  $S = 1/2$  staggered magnetic moment is generated on the Cu ions in the vicinity of the impurity sites [1–8]. Below the superconducting transition temperature, the moment is partially screened in optimally doped YBCO, but remains unscreened down to the lowest temperatures in the underdoped regime [3,2]. Low-temperature STM experiments [9] have directly observed the local electronic structure around the Zn impurity atoms on the surface of superconducting  $\text{Bi}_2\text{Sr}_2\text{CaCu}_2\text{O}_{8+x}$  (BSCCO). The tunneling differential conductance above the Zn site exhibits a sharp in-gap resonance peak near zero bias ( $-1.5\text{meV}$ ) for electrons tunneling out of the sample [9].

While the presence of a resonance impurity state is consistent with the strong local potential scattering near the impurity [10], the latter does not account for the local magnetic moment induced by nonmagnetic impurities observed by NMR. This has led to attempts to identify the low energy conductance peak with the Kondo resonance resulting from the Kondo screening of the local moment by the superconducting (SC) electrons [12]. However, the *formation* of the local moment itself near nonmagnetic impurities in a d-wave superconductor has not been addressed. In this paper, we present a theory which simultaneously explains the local moment formation and predicts a strong low energy resonance in the local density of states (LDOS) spectrum. Furthermore, it can account for the observed particle-hole asymmetry in the spatially averaged STM spectrum which is difficult to explain by purely potential scattering [11].

We study the local moment formation in d-wave superconductors in proximity to Mott insulators. In the resonance-valence-bond (RVB) picture [13], the electrons

are paired into spin singlets, which are mobilized by the doped holes and condense into the SC state below  $T_c$ . A nonmagnetic impurity atom such as Zn/Li or a Cu vacancy locally breaks a singlet, creating an unpaired spin. This extra  $S = 1/2$  moment can be self-consistently trapped by the local impurity potential, forming a local moment confined to the neighboring sites of the impurity. Our strategy is as follows. The d-wave BCS ground state  $|\text{BCS}\rangle$  is a spin singlet and the low-lying excitations are the nodal quasiparticles. A single quasiparticle excitation,  $\gamma^\dagger|\text{BCS}\rangle$ , carries a spin  $S = 1/2$ . The unpaired spin induced by the impurity corresponds to a superposition of such one- $\gamma$  excitations. We refer to such a doublet state as a  $\gamma\text{BCS}$  state. If the self-consistently determined energy of the  $\gamma\text{BCS}$  state is lower than that of the BCS ground state, the true ground state is a doublet with a net  $S = 1/2$  moment. Below, we show that the physical picture described above can be realized by a renormalized slave boson meanfield theory of the  $t - J$  model. We carry out fully self-consistent, spatially unrestricted calculations of the valence bond, SC order parameter, local doping concentration (LDC), and the spin density distribution in the doublet  $\gamma\text{BCS}$  state and compare its energy to that of the singlet d-wave BCS state. We find that binding occurs and the doublet  $\gamma\text{BCS}$  state becomes the true ground state when the renormalized exchange coupling  $\alpha J$  exceeds a nonzero doping dependent critical value due to the linearly vanishing quasiparticle density of states. The  $S = 1/2$  moment exhibits a staggered pattern localized around the impurity in agreement with the results derived from the NMR experiments. We determine the phase boundary in the  $\alpha J$  versus doping plane, obtain the tunneling density of states in the doublet  $\gamma\text{BCS}$  state and compare to the results of STM experiments.

We begin with the  $t - J$  model on a square lattice in the presence of the long-range Coulomb interaction,

$$H = - \sum'_{i,j} (t_{ij} c_{i\sigma}^\dagger c_{j\sigma} + \text{h.c.}) + J \sum'_{\langle i,j \rangle} (\mathbf{S}_i \cdot \mathbf{S}_j - \frac{1}{4} n_i n_j) + \frac{V_c}{2} \sum'_{i \neq j} \frac{n_j - \bar{n}}{|\mathbf{r}_i - \mathbf{r}_j|} n_i - \mu \sum_i n_i. \quad (1)$$

Here  $c_{i\sigma}^\dagger$  creates an electron and the spin operator  $\mathbf{S}_i = (\frac{1}{2}) c_{i\alpha}^\dagger \vec{\sigma}_{\alpha\beta} c_{i\beta}$ . The sum over  $i, j$  in the hopping term includes the nearest neighbors (n.n.) where  $t_{ij} \equiv t$  and the next n.n. where  $t_{ij} \equiv t'$ . To model a nonmagnetic impurity or a Cu defect, we remove a site on the  $L \times L$  square lattice as indicated by the primes on the summations in Eq. (1). The total number of sites is then  $N_s = L \times L - 1$ . The long-range Coulomb interaction strength  $V_c$  in Eq. (1) is given by  $V_c = e^2/4\pi\epsilon a \sim t$  [14]. Eq. (1) is only physical in the limit of strong on-site Coulomb repulsion, i.e. under the constraint of no double occupancy,  $n_i = c_{i\sigma}^\dagger c_{i\sigma} \leq 1$ . Such a projected Hilbert space can be treated in the slave-boson formulation by writing  $c_{i\sigma}^\dagger = f_{i\sigma}^\dagger b_i$ , where  $f_{i\sigma}^\dagger$  is a spin-carrying fermion and  $b_i$  a spinless boson [15] with the constraints  $f_{i\sigma}^\dagger f_{i\sigma} + b_i^\dagger b_i = 1$ . The AF spin-exchange term is decoupled according to [16]

$$\mathbf{S}_i \cdot \mathbf{S}_j = -\frac{3}{8} [\chi_{ij}^* f_{i\sigma}^\dagger f_{j\sigma} + \Delta_{ij}^* (f_{i\downarrow} f_{j\uparrow} - f_{i\uparrow} f_{j\downarrow}) + \text{h.c.}] + \frac{3}{8} (|\chi_{ij}|^2 + |\Delta_{ij}|^2),$$

where  $\Delta_{ij}$  and  $\chi_{ij}$  are the pairing and valence bond order parameters on each n.n. bond respectively,

$$\Delta_{ij} = \langle f_{i\downarrow} f_{j\uparrow} - f_{i\uparrow} f_{j\downarrow} \rangle, \quad \chi_{ij} = \langle f_{i\sigma}^\dagger f_{j\sigma} \rangle. \quad (2)$$

In the meanfield SC state, the bosons locally condense [14,15] into the coherent state,

$$|\Psi_b\rangle = A e^{\sum_i \phi_i b_i^\dagger} |0\rangle, \quad A = e^{-\frac{1}{2} \sum_i |\phi_i|^2}. \quad (3)$$

The LDC is given by  $x_i = \langle \Psi_b | b_i^\dagger b_i | \Psi_b \rangle = |\phi_i|^2$ . The constraint  $|\phi_i|^2 = 1 - n_i^f$  is enforced on average at every site by locally adjusting the chemical potential.

The effects of fluctuation mediated spin-spin interaction can be taken into account in the renormalized mean-field theory by including an interaction term,

$$H_\alpha = \alpha J \sum'_{\langle i,j \rangle} \langle \mathbf{S}_i \rangle \cdot \mathbf{S}_j, \quad (4)$$

where  $\alpha$  is a phenomenological parameter between zero and one. A similar approach was used recently for a successful description of the spin dynamics in YBCO [16], including the “41 meV” resonance and the incommensurate structures observed by inelastic neutron scattering. In that case, the renormalized meanfield theory facilitated an RPA-type calculation of the magnetic susceptibility in linear response. In the presence of the impurity,

we study the fully self-consistent, spatially unrestricted solution which includes the nonlinear effects induced by  $H_\alpha$  near the impurity.

We diagonalize the theory in real space by writing

$$\{f_{i\uparrow}^\dagger(t), f_{i\downarrow}(t)\} = \sum_n \{u_{ni}, v_{ni}\} \gamma_n^\dagger e^{-iE_n t/\hbar}, \quad (5)$$

where  $\gamma_n^\dagger$ ,  $n = 1, \dots, 2N_s$  creates a Bogoliubov quasiparticle with energy  $E_n$  and wave-function  $(u_{ni}, v_{ni})$  as solutions of the Bogoliubov-de Gennes (BdG) equations. Since the particle-hole symmetry in the quasiparticle excitation spectrum, which reflects the degeneracy in spin excitations, is broken in the presence of a net spin moment, we keep all independent eigenstates with  $E_n < 0$  and  $E_n > 0$  and construct the ground state according to the occupation of the fermionic quasiparticle orbitals:

$$|\Psi_G, n_{\text{occ}}\rangle = \prod_{n=1}^{n_{\text{occ}}} \gamma_n^\dagger |0\rangle = \prod_n \sum_{i=1}^{N_s} [u_{ni}^* f_{i\uparrow}^\dagger + v_{ni}^* f_{i\downarrow}] |0\rangle, \quad (6)$$

where  $n_{\text{occ}}$  labels the last  $\gamma$ -quasiparticle level to be occupied. The spin-singlet d-wave BCS state corresponds to  $|\text{BCS}\rangle = |\Psi_G, n_{\text{occ}} = N_s\rangle$ , whereas the  $\gamma$ BCS state is given by  $|\gamma\text{BCS}\rangle = |\Psi_G, n_{\text{occ}} = N_s + 1\rangle$ , which is a global doublet with a net  $S = 1/2$  moment. These states must be determined by minimizing  $\langle \Psi_G, n_{\text{occ}} | H_{\text{mf}} + H_\alpha | \Psi_G, n_{\text{occ}} \rangle$ , leading to the self-consistency equations

$$\Delta_{ij} = \sum_{n=n_{\text{occ}}+1}^{2N_s} v_{ni}^* u_{nj} - \sum_{n=1}^{n_{\text{occ}}} u_{ni} v_{nj}^*, \quad (7)$$

$$\chi_{ij} = \sum_{n=n_{\text{occ}}+1}^{2N_s} v_{ni}^* v_{nj} + \sum_{n=1}^{n_{\text{occ}}} u_{ni} u_{nj}^*. \quad (8)$$

The LDC and the local spin density are given by

$$x_i = 1 - \sum_{n=n_{\text{occ}}+1}^{2N_s} |v_{ni}|^2 - \sum_{n=1}^{n_{\text{occ}}} |u_{ni}|^2, \quad (9)$$

$$S_i^z = \frac{1}{2} \left[ \sum_{n=1}^{n_{\text{occ}}} |u_{ni}|^2 - \sum_{n=n_{\text{occ}}+1}^{2N_s} |v_{ni}|^2 \right]. \quad (10)$$

For  $|\Psi_G, n_{\text{occ}}\rangle$  to be a self-consistent ground state, it requires a lowest total energy and, in addition,  $E_{n_{\text{occ}}} < 0$ .

The BdG equation and the spatially unrestricted self-consistency equations can be solved by numerical iterations. We use  $J$  as the unit of energy and set  $t/J = 3$ ,  $V_c/J = 5$ . The impurity/defect is located at  $(L/2, L/2)$ . We first consider  $t' = 0$  and focus on the nature of the ground state. The energies per site for the BCS and the  $\gamma$ BCS states are shown in Fig. 1 as a function of the renormalized spin-spin interaction  $\alpha J$  for  $L = 24$  at an average doping  $x = 0.14$ . While that of the singlet state is independent of  $\alpha J$ , the energy of the doublet  $\gamma$ BCS-state is reduced with increasing  $\alpha J$  and drops abruptly

below that of the singlet state near a critical value  $\alpha_c$ , indicating that the doublet state can gain substantial spin-exchange energy through the formation of the magnetic moment. To determine the value of  $\alpha_c$  at which a phase transition into the  $\gamma$ BCS-state occurs, we calculate the energy of the  $n_{\text{occ}} = N_s + 1$ -th  $\gamma$ -quasiparticle level  $E_{n_{\text{occ}}}$  as a function of  $\alpha J$  and identify  $\alpha_c \simeq 0.68$  at  $x = 0.14$  by the point where it crosses the Fermi energy. The phase diagram in the plane of  $\alpha J$  versus doping  $x$  is plotted in the inset of Fig. 1, which shows that the formation of the local moment requires a smaller renormalized spin interaction in the underdoped regime.

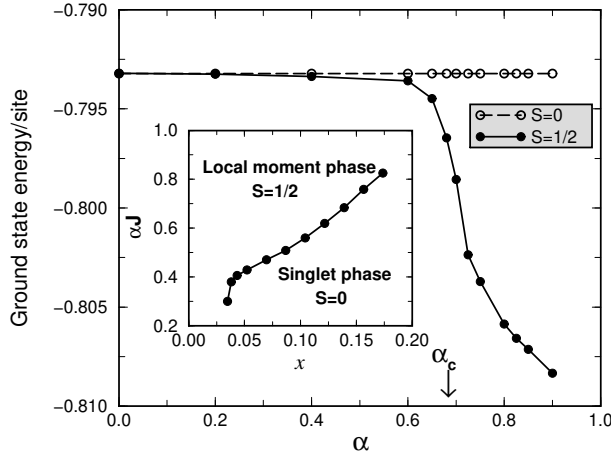


FIG. 1. Energy per site of the singlet and the doublet states as a function of  $\alpha J$  on a  $24 \times 24$  lattice at  $x = 0.14$ . The critical value of the exchange coupling is  $\alpha_c \simeq 0.68$ . Inset: phase diagram in the  $\alpha J$  versus doping  $x$  plane.

Next, we turn to the spatial distribution of the impurity/defect induced local moment in the  $\gamma$ BCS-state. We choose large systems with  $L = 32$  and set  $t' = -t/3$  and  $\alpha = 0.75 > \alpha_c$  at  $x = 0.14$ . The self-consistent solutions of the LDC  $x_i$  and the d-wave gap amplitude,  $\Delta_i^d = (\Delta_{i,i+\hat{x}} + \Delta_{i,i-\hat{x}} - \Delta_{i,i+\hat{y}} - \Delta_{i,i-\hat{y}})/4$ , are shown in Figs. 2a and 2b as 2D maps. Both  $x_i$  and  $\Delta_i^d$  are strongly suppressed in the vicinity of the impurity/defect, but quickly resume their bulk values away from it. The spatial distribution of the magnetic moment  $S_i^z$ , having a net magnitude  $\sum_i S_i^z = 1/2$ , is plotted in Fig. 2c. It shows a staggered pattern localized around the impurity in good agreement with that derived from the NMR experiments [2,3]. The majority of the net moment resides on the four nearest neighbors of the impurity. Interestingly, along the nodal directions (diagonals) of the d-wave gap, weak incommensurate spin density wave (SDW) oscillations arise with a periodicity of approximately 8 unit cells. This feature is more clearly seen in the 3D plot of the *staggered* magnetic moment shown in Fig. 2d. The dependence of the SDW periodicity on the value of  $t'$  and the doping  $x$  is consistent with the behavior of the

bulk spin susceptibility which peaks around similar incommensurate wave-vectors [16]. Physically, an impurity/defect induces a local moment in its immediate vicinity, which subsequently leaks into the bulk via the short-range spin-spin correlation in the short-range RVB state.

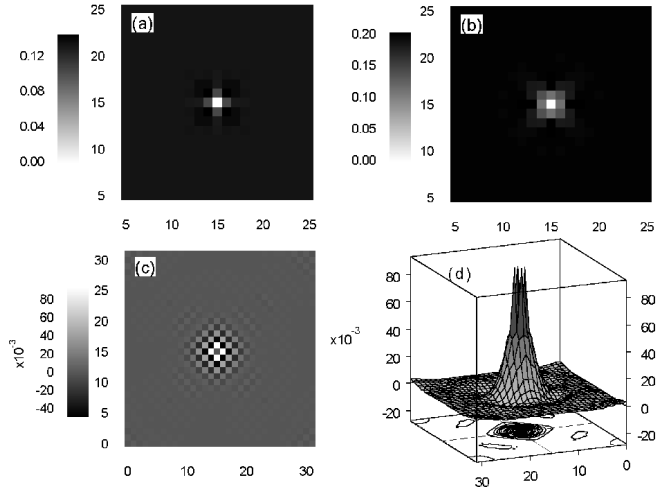


FIG. 2. Self-consistent solution of the  $\gamma$ BCS-state with a net  $S = 1/2$  local moment on a  $32 \times 32$  lattice with  $\alpha = 0.75 > \alpha_c$  and  $t' = -t/3$ . The impurity/defect is located at  $(15, 15)$ . (a) LDC  $x_i$ . (b) d-wave gap amplitude  $\Delta_i^d$ . (c) Distribution of the local moment  $S_i^z$ . (d) 3D-plot of the *staggered* magnetic moment.

We next study the LDOS spectrum measured by STM. Note that the net spin polarization in the doublet ground state flips between  $S_z = \pm 1/2$ , which should be identified with the two degenerate states of an  $S = 1/2$  quantum impurity. We set  $S_z = 1/2$  and do not consider here the effect of Kondo coupling between such an extended local moment and the quasiparticles which can be quite different from the conventional Kondo problem in d-wave superconductors. The spectral weight of the electron is a product of those associated with the boson and fermion states given in Eqs. (3) and (5) respectively. We derive the LDOS for the up and down spin electrons,

$$N_{i\uparrow}(\omega) = \left[ \sum_n^{n_{\text{occ}}} A_{n\uparrow}^- |u_{ni}|^2 + \sum_{n=n_{\text{occ}}+1}^{2N_s} A_{n\uparrow}^+ |u_{ni}|^2 \right] \delta(\omega - E_n)$$

$$N_{i\downarrow}(\omega) = \left[ \sum_n^{n_{\text{occ}}} A_{n\downarrow}^+ |v_{ni}|^2 + \sum_{n=n_{\text{occ}}+1}^{2N_s} A_{n\downarrow}^- |v_{ni}|^2 \right] \delta(\omega + E_n),$$

where  $A_{n\sigma}^\pm$  is the boson coherent state overlap for adding (+) or removing (−) an electron with spin- $\sigma$  accompanied by adding/removing a  $\gamma$ -quasiparticle from the  $n$ -th fermionic orbital. In order to maintain the occupation constraint in the final states, the corresponding boson coherent states, defined as  $\phi_{in\sigma}^\pm$ , must satisfy  $(\phi_{in\uparrow}^\pm)^2 = (\phi_{in\downarrow}^\mp)^2 = \phi_i^2 \pm |u_{ni}|^2 \mp |v_{ni}|^2$ . Using Eq. (3), we obtain the spectral weight for the bosons,

$$A_{n\uparrow(l)}^+ = \phi_i^2 e^{-2 \sum_i [\phi_i - \phi_{in\uparrow(l)}^+]^2},$$

$$A_{n\uparrow(l)}^- = [\phi_{in\uparrow(l)}^-]^2 e^{-2 \sum_i [\phi_i - \phi_{in\uparrow(l)}^-]^2}.$$

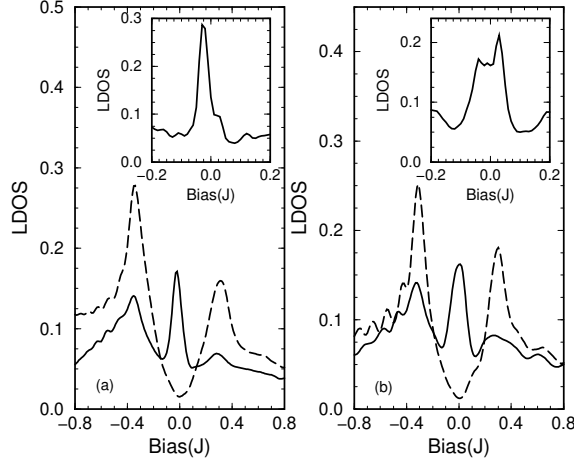


FIG. 3. The LDOS spectra at the n.n. sites of the impurity/defect (solid lines) and near the corner (dashed lines) of  $32 \times 32$  lattices at  $x = 0.14$ . (a)  $t' = -0.45t$  and  $\alpha J = 0.7$ , close to the phase boundary. (b)  $t' = -t/3$  and  $\alpha J = 0.75$ , the same system as in Fig. 2. Insets: details of the resonance line-shape near zero bias with reduced thermal broadening.

Due to the localized nature of the impurity states, the order parameters in Eqs. (7-10) are insensitive to the boundary conditions for large system sizes. We have calculated  $N_i(\omega)$  on  $32 \times 32$  lattices and averaged the results over a set of different boundary conditions to reduce the finite-size effects. In Fig. 3, we plot the LDOS as a function of the bias voltage for two ground states, one is close to the phase boundary (Fig. 3a) and the other (Fig. 3b) is the same system used in Fig. 2 in the local moment phase. On the n.n. site of the impurity/defect, the LDOS (solid lines) exhibits a near zero-bias resonance with its peak located on the occupied side of the spectrum. Comparing to the LDOS obtained near the corner of the system (dashed lines), the coherence peaks at the gap edges have been strongly suppressed around the impurity/defect. These results are in good agreement with STM observations [9]. The LDOS spectra with reduced thermal broadening are plotted in the insets of Fig. 3 to reveal the details of the resonance line-shape. The inset in Fig. 3a is in good agreement with experiments. However, comparison with the inset in Fig. 3b shows that the resonance line-shape is sensitive to the parameters and show several peaks asymmetrically distributed around zero bias. The low energy spectra can be qualitatively understood by considering the last two occupied quasi-particle levels:  $E_{N_s}$  and  $E_{N_s+1}$ . The resonance state at these two energies is occupied in the local moment phase which should in principle lead to four resonance

peaks centered at  $\pm E_{N_s}$  and  $\pm E_{N_s+1}$  in the LDOS spectrum through their particle-hole reflections. However, since the SC coherence is significantly reduced near the impurity/defect, the spectral weights have the property  $|u_{N_s}|^2 \gg |v_{N_s}|^2$  whereas  $|u_{N_s+1}|^2 \ll |v_{N_s+1}|^2$  leading to two predominant peaks near zero bias. The peak at the negative energy  $E_{N_s}$  (positive energy  $|E_{N_s+1}|$ ) corresponds to removing (adding) an up (down) spin electron from the resonance state. Since the resonance state is strongly localized, its LDOS resides mainly on the n.n. sites and remains particle-hole asymmetric upon spatial averaging near the impurity. This is in contrast to pure potential scattering models [11].

The existence of the low energy resonance is a robust feature of our model, even though the detailed structure of the resonance may vary. Since recent STM data on BSCCO surface revealed a spatially inhomogeneous electronic structure [17] that can be interpreted as off-stoichiometry carrier doping induced spatial variations in the LDC [14], the present theory would predict a distribution of the resonance structure over different Zn-impurity sites. A systematic study of the distribution of the impurity/defect induced conductance peaks and its correlation to the inhomogeneity exhibited by the local electronic structure would be very desirable.

We thank X. Dai, E. Hudson, and S.-H. Pan for useful discussions. P.A.L is supported by NSF Grant No. DMR-9813764 Z.W. is supported by DOE Grant No. DE-FG02-99ER45747 and an award from Research Corporation.

- 
- [1] J. Bobroff et. al., Phys. Rev. Lett. **83**, 4381 (1999).
  - [2] M.-H. Julien et. al., Phys. Rev. Lett. **84**, 3422 (2000).
  - [3] J. Bobroff et. al., Phys. Rev. Lett. **86**, 4116 (2001).
  - [4] A. V. Mahajan et. al., Phys. Rev. Lett. **72**, 3100 (1994); Eur. Phys. J. B**13**, 457 (2000).
  - [5] P. Mendels et. al., Europhys. Lett. **46**, 678 (1999).
  - [6] W. A. MacFarlane et al., Phys. Rev. Lett. **85**, 1108 (2000).
  - [7] A. M. Finkelstein et al., Physica C**168**, 370 (1990).
  - [8] R. Kilian, et. al. Phys. Rev. B**59**, 14432 (1999).
  - [9] S. H. Pan et al., Nature **403**, 746 (2000).
  - [10] M. I. Salkola, A. V. Balatsky, and D. J. Scalapino, Phys. Rev. Lett. **77**, 1841 (1996).
  - [11] M. E. Flatté, Phys. Rev. B**61**, 14920 (2000).
  - [12] A. Polkovnikov, S. Sachdev, and M. Vojta, Phys. Rev. Lett. **86**, 296 (2001).
  - [13] P. W. Anderson, Science **235**, 1196 (1987).
  - [14] Z. Wang, et. al., Phys. Rev. B**65**, 064509 (2002).
  - [15] G. Kotliar and J. Liu, Phys. Rev. B**38**, 5142 (1988); G. Baskaran, Z. Zou, and P. W. Anderson, Solid State Commun. **63**, 973 (1987).
  - [16] J. Brinckmann and P. A. Lee, Phys. Rev. Lett. **82**, 2915 (1999); Phys. Rev. B**65**, 014502 (2002).
  - [17] S. H. Pan et al., Nature **413**, 282 (2001).